Received 3 March; accepted 22 June 1998.

1. Blanchard, M. B., Brownlee, D. E., Bunch, T. E., Hodge, P. W. & Kyte, F. T. Meteoroid ablation spheres from deep-sea sediments. *Earth Planet. Sci. Lett.* **46,** 178–190 (1980).
2. Taylor, S. & Brownlee, D. E. Cosmic spherules in the geologic record. *Meteoritics* **26,** 203–211 (1991).
3. Brownleee, D. E., Bates, B. & Schramm, L. The elemental composition of stony cosmic spherules. *Meteoritics Planet. Sci.* **32,** 157–175 (1997).
4. Brownlee, D. E. in *The Sea* Vol. 7 (ed. Emilinani, C.) 733–762 (Wiley, New York, 1981).
5. Brownlee, D. E. Cosmic dust: collection and research. *Annu. Rev. Earth Planet. Sci.* **13,** 147–173 (1985).
6. Maurette, M., Jéhanno, C., Robin, E. & Hammer, C. Characteristics and mass distribution of extraterrestrial dust from the greenland ice cap. *Nature* **328,** 699–702 (1987).
7. Robin, E., Christophe Michel-Levy, N., Bourot-Denise, M. & Jéhanno, C. Crystalline micrometeorites from Greenland blue lakes: their chemical composition, mineralogy and possible origin. *Earth Planet. Sci. Lett.* **97,** 162–176 (1990).
8. Maurette, M. *et al.* A collection of diverse micrometeorites recovered from 100 tonnes of Antarctic blue ice. *Nature* **351,** 44–46 (1991).
9. Taylor, S., Lever, J. H. & Harvey, R. P. Accretion rate of cosmic spherules measured at the South Pole. *Nature* **392,** 899–902 (1998).
10. Robin, E., Bontè, Ph., Froget, L., Jéhanno, C. & Rocchia, R. Formation of spinels in cosmic objects during atmospheric entry: A clue to the Cretacious-Tertiary boundary event. *Earth Planet. Sci. Lett.* **108,** 181–190 (1992).
11. Gayraud, J., Robin, E., Rocchia, R. & Froget, L. Formation conditions of oxidized Ni-rich spinel and their relevance to the K/T boundary event. *Geol. Soc. Am. Spec. Pap.* **307,** 425–443 (1996).
12. Brownlee, D. E., Bates, B. A. & Wheelock, M. M. Extraterrestrial platinum group nuggets in deep-sea sediments. *Nature* **309,** 693–695 (1984).
13. Suominen, V. The chronostratigraphy of southwestern Finland, with special reference to Postjotnian and Subjotnian diabases. *Geol. Surv. Fin. Bull.* **304** (1991).
14. Amatov, A., Laitakari, I. & Prooshin, Ye. in *Explanation to the Map of Precambrian Basement of the Gulf of Finland and Surrounding Area 1:1 mil* (ed. Koistinen, T.) *Geol. Surv. Finl. Spec. Pap.* **21,** 99–113 (1996).
15. Neuvonen, K. J. Remanent magnetization of the Jotnian sandstone in Satakunta, SW-Finland. *Bull. Geol. Soc. Fin.* **45,** 23–27 (1973).
16. Marttila, E. Satakunnan hiekkakiven sedimentaatio-olosuhteista. (On the sedimentary environment of the Satakunta sandstone.) Thesis, Univ. Turku (1969).
17. Kohonen, J., Pihlaja, P., Kujala, H. & Marmo, J. Sedimentation of the Jotnian Satakunta sandstone, western Finland. *Geol. Surv. Fin. Bull.* **369** (1993).
18. Des Marais, D. J., Strauss, H., Summons, R. E. & Hayes, J. M. Carbon isotope evidence for the stepwise oxidation of the Proterozoic environment. *Nature* **359,** 605–609 (1992).
19. Kasting, J. F. Earth's early atmosphere. *Science* **259,** 920–926 (1993).
20. Ohmoto, H. When did the Earth's atmosphere become oxic? *Geochem. News* **93,** 12–27 (1997).
21. Jéhanno, C., Boclet, D., Bonté, Ph., Castellarin, A. & Rocchia, R. Identification of two populations of extraterrestrial particles in a Jurassic hardground of the Southern Alps. *Proc. Lunar Planet. Sci. Conf.* **18,** 623–630 (1988).
22. Marttila, E. Mikrometeorlitteja Satakunnan kiekkakivessä. (Micrometeorites in the Satakunta sandstone.) *Geologi* **20,** 135–136 (1968).
23. Steele, I. M. Olivine in Antarctic micrometeorites: Comparison with other extraterrestrial olivine. *Geochim. Cosmochim. Acta* **56,** 2923–2929 (1992).
24. Beckerling, W. & Bischoff, A. Occurrence and composition of relict minerals in micrometeorites from Greenland and Antarctica—Implication for their origins. *Planet. Space Sci.* **43,** 435–449 (1995).
25. Brownlee, D. E., Bates, B. & Beauchamp, R. H. in *Chondrules and their Origin* (ed. King, E. A.) 122–133 (Lunar and Planetary Inst., Houston, 1983).
26. Love, S. G. & Brownlee, D. E. Heating and thermal transformation of micrometeoroids entering the Earth's atmosphere. *Icarus* **89,** 26–43.
27. Thorslund, P. & Wickman, F. E. Middle Ordovician chondrite in fossiliferous limestone from Brunflo, central Sweden. *Nature* **289,** 285–286 (1981).
28. Goodwin, A. M. *Precambrian Geology; the Dynamic Evolution of the Continental Crust* (Academic, San Diego, 1991).
29. Bence, A. E. & Albee, A. L. Empirical correction factors for the electron microanalysis of silicates and oxides. *J. Geol.* **76,** 382–403 (1968).
30. Kerridge, J. F. & Matthews, M. S. (eds) *Meteorites and the Early Solar System* Appendix 3 (Univ. Arizona Press, Tucson, 1988).

Acknowledgements. We thank T. Grund, F. Bartschat, U. Heitmann, M. Flucks and D. Kettrup for technical assistance, and A. Bischoff, E. Marttila, A. Putnis, U. Schärer, and H. Strauss for discussions. Field work was supported by a DAAD-Finish Academy of Science exchange program (A.D. and L.J.P.) and we acknowledge additional support by DFG.

Correspondence and requests for materials should be addressed to A.D. (e-mail: deutsca@ uni-muenster.de).

Magnetic trapping of calcium monohydride molecules at millikelvin temperatures

Jonathan D. Weinstein*, Robert deCarvalho*, Thierry Guillet*, Bretislav Friedrich*† & John M. Doyle*

** Department of Physics, † Department of Chemistry, Harvard University, Cambridge, Massachusetts 02138, USA*

Recent advances[1–5] in the magnetic trapping and evaporative cooling of atoms to nanokelvin temperatures have opened important areas of research, such as Bose–Einstein condensation and ultracold atomic collisions. Similarly, the ability to trap and cool molecules should facilitate the study of ultracold molecular physics and collisions[6]; improvements in molecular spectroscopy could be anticipated. Also, ultracold molecules could aid the search for electric dipole moments of elementary particles[7]. But although laser cooling (in the case of alkali metals[1,8,9]) and cryogenic surface thermalization (in the case of hydrogen[10,11]) are currently used to cool some atoms sufficiently to permit their loading into magnetic traps, such techniques are not applicable to molecules, because of the latter's complex internal energy-level structure. (Indeed, most atoms have resisted trapping by these techniques.) We have reported a more general loading technique[12] based on elastic collisions with a cold buffer gas, and have used it to trap atomic chromium and europium[13,14]. Here we apply this technique to magnetically trap a molecular species—calcium monohydride (CaH). We use Zeeman spectroscopy to determine the number of trapped molecules and their temperature, and set upper bounds on the cross-sectional areas of collisional relaxation processes. The technique should be applicable to many paramagnetic molecules and atoms.

Evaporative cooling has proved to be a powerful technique for producing ultracold atoms[9,15,16]. To employ evaporative cooling, atoms are first loaded into a magnetic trap. Although laser cooling is commonly used to load Li, Na, Rb and Cs, extension of this method to molecules is precluded by their complex internal level structure. (A technique to use multiline Raman cell radiation to optically cool alkali-metal dimers has been proposed, but not yet implemented[17].) Hydrogen has also been trapped but is the only atoms that can be loaded by surface thermalization, as its very low binding energy to liquid helium (1 K) is unique. A molecule would be strongly adsorbed by such a cold surface. A different approach to produce cold molecules for trapping is photoassociation of laser-cooled alkali-metal atoms[18,19]. This technique has recently been demonstrated[20], producing Cs_2 molecules at a translational temperature of 300 μK. This is sufficiently cold that it should be possible to trap these molecules with far-off-resonance optical trapping

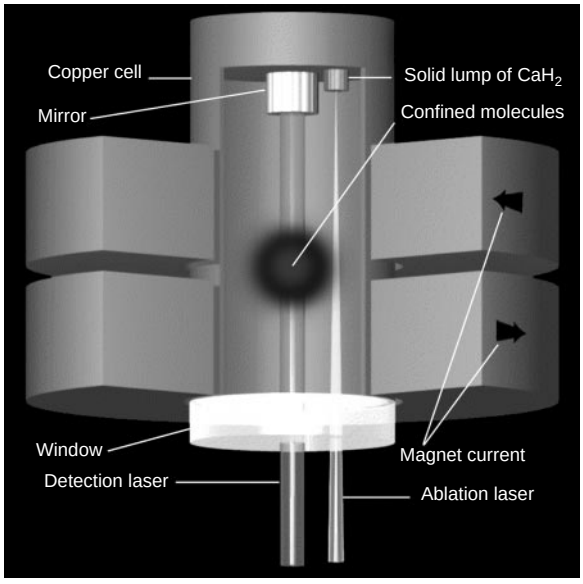

Figure 1 Cutaway diagram of the experimental apparatus. The copper cell is anchored to the mixing chamber of a dilution refrigerator. The magnet is immersed in liquid helium. A vacuum space isolates the relatively warm (4 K) magnet from the cold (300 mK) cell. The superconducting magnet coils are arranged in the anti-Helmholtz configuration (currents travel in opposite directions) and generate a spherical quadrupole magnetic trap up to 3 T deep. For the 1 μ_B magnetic moment of the ground state of CaH, this results in a trap depth of 2 K. Detection and ablation lasers enter through three borosilicate windows (not shown) at 300 K, 77 K and 4 K before passing through the fused silica window at the bottom of the cell. Fluorescence from the trapped molecules (induced by the detection laser) is collected outside the 300 K window by a photomultiplier tube.

techniques[21–24]. We are aware of work where internally excited, translationally cold Cs_2 molecules have been produced and trapped in this manner[25].

In an attempt to broaden the range of atoms that can be trapped, and to trap molecules, we developed a general trap loading technique[12] that relies only on elastic collisions with a cold buffer gas of helium. A cryogenically cooled buffer gas thermalizes atoms or molecules to temperatures less than the depth of the trap.

We chose to trap CaH because it is a paramagnetic molecule that has been previously studied and analysed at zero field. CaH has a magnetic moment of 1 Bohr magneton ($1\,\mu_B$) in the ground state. Also, its relatively simple structural and spectroscopic properties aid in detection. Finally, it was straightforward to produce CaH via laser ablation, a process particularly well suited to our cryogenic environment.

The principles of buffer-gas loading and the specifics of our apparatus are given elsewhere[12,13]. Briefly, our trap is a magnetic potential with a magnetic-field minimum in free space. This field minimum attracts molecules in the low-field-seeking state (that is, those with their magnetic moments orientated anti-parallel to the magnetic field), and repels strong-field-seeking molecules. Our magnetic trap is a spherical quadrupole field (see Fig. 1). Although particles in such a trap are subject to non-adiabatic spin flip (Majorana) losses near the trap centre, our trap parameters are such that these losses are negligible during our observation time[26,27].

CaH is produced, thermalized, and trapped within a copper cell inside the bore of the magnet. The cell is maintained at cryogenic temperatures (typically 300 mK) by a dilution refrigerator. The cell is filled with ^{3}He gas (typically at densities of $2 \times 10^{16}\,cm^{-3}$). CaH is created via laser ablation of a solid sample of CaH_2 near the edge of the trap potential. A fused-silica window on the bottom of the cell permits optical access for the ablation beam, as well as a probe laser beam used to detect the molecules. Typically, a 10 mJ laser pulse (5 ns long) at 532 nm is used to ablate solid CaH_2 and produce molecular CaH. The CaH molecules diffuse through the helium gas, and elastic collisions between the CaH and the helium gas thermalize the translational temperature of the molecules to that of the helium. The cold molecules in the weak-field-seeking states are confined by the magnetic fields and trapped. However, because these trapped molecules are thermally distributed, they evaporate over the edge of the trap at a rate dependent on the ratio of the trap depth to the translational temperature of the molecules.

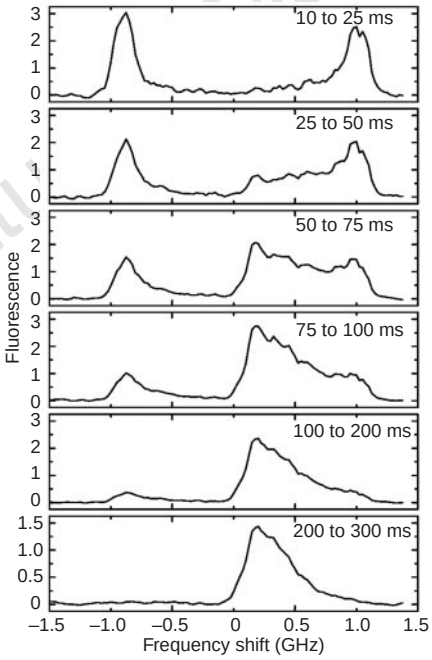

Figure 2 Time evolution of the CaH spectrum. The data were obtained by firing a single ablation pulse and monitoring the fluorescence as a function of time at a single probe frequency. The process was repeated at different frequencies, and the fluorescence averaged over the specified time window in order to obtain the spectra. Times quoted are relative to the ablation pulse. These spectra reveal that high-field-seekers (at negative frequency shifts) quickly leave the trap. The trapped low-field-seekers (positive frequency shifts) are confined and compressed towards the centre of the trap.

The CaH molecules are detected by laser fluorescence spectroscopy. They are excited on the $|B^2\Sigma, \nu' = 0) \leftarrow |X^2\Sigma, \nu'' = 0\rangle$ transition at 634 nm (refs 28, 29). The fluorescence emitted on the $|B^2\Sigma, \nu' = 0) \rightarrow |X^2\Sigma, \nu'' = 0\rangle$ transition at 690 nm is detected with a photomultiplier tube (here ν is the vibrational quantum number of the CaH state and $'('')$ designates the excited (ground) state). Colour filters are used to block the scattered probe radiation (634 nm) and pass the frequency-shifted fluorescence (690 nm). The Franck–Condon factor for the $\nu' = 0 \rightarrow \nu'' = 1$ decay has been calculated[30] to be 0.028. In order to determine the absolute number of molecules, we calibrate our fluorescence spectroscopy with absorption spectroscopy[31]. We found that under certain conditions 10^{10} ground-state CaH molecules could be produced in a single ablation pulse.

The ground-state molecules are detected on the $|N' = 1, J' = 3/2, \nu' = 0\rangle \leftarrow |N'' = 0, J'' = 1/2, \nu'' = 0\rangle$ transition (N, J, and M_J are the rotational, angular momentum, and projection of angular momentum quantum numbers, respectively). In a magnetic field, this transition is observed to split into multiple features. The detection and analysis presented here was performed on the two slightly broadened features which undergo opposite frequency shifts in a magnetic field. The measured shifts of these features are linear in field and indicate a small difference ($0.02\,\mu_B$) in the magnetic moments of the ground and excited states. A theoretical analysis (B.F. *et al.*, manuscript in preparation) indicates that the feature shifted towards higher frequencies is the transition from the $|N'' = 0, J'' = 1/2, M''_J = 1/2\rangle$ low-field-seeking state to the $|N' = 1, J' = 3/2, M'_J = 3/2\rangle$ excited state, and the feature that shifts towards lower frequencies is the transition from the $|N'' = 0, J'' = 1/2, M''_J = -1/2\rangle$ high-field-seeking state to the $|N' = 1, J' = 3/2, M'_J = -3/2\rangle$ excited state. The magnetic splitting observed is largely due to a perturbation of the excited state by a nearby $A^2\Pi, \nu = 1$ state, which is $13\,cm^{-1}$ above the $|N' = 1, J' = 3/2\rangle$ state[28,29].

Figure 2 displays spectra of these features taken at various times after the ablation pulse. The magnetic trap depth is 3 T, and the cell temperature is 275 ± 10 mK before the ablation pulse. Knowledge of the frequency shift as a function of field (in addition to the field

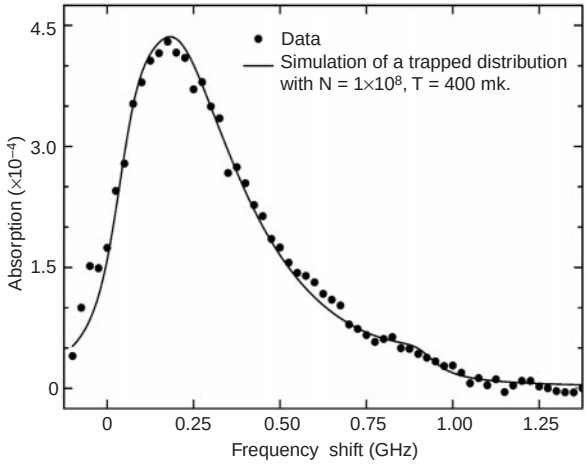

Figure 3 Fit of CaH spectrum to a thermal distribution of trapped atoms. Data were taken with a 3 T trap depth and a cell temperature of 300 mK before ablation, and were taken from 200 ms to 300 ms after the ablation pulse. This fit determined the number and temperature of trapped CaH molecules to be $N = 1 \times 10^8$ and $T = 400$ mK.

distribution, selection rules, and probe beam geometry) allows the determination, from the data, of the distribution of the low-field and high-field seeking states of CaH in the magnetic field. Because the shift is linear in field (over the range of fields in our trap), the magnitude of the frequency shift of the observed transition of a CaH molecule is simply proportional to the field it is in. Analysis of our data confirms that the transitions originating from the low-field-seeking state and the high-field-seeking state are shifted to lower frequencies (the left-hand side of our spectra) and higher frequencies (the right-hand side), respectively.

As can be seen in Fig. 2, the spectrum is initially nearly symmetric, indicating that at short times after the production of CaH, the distribution of the high-field-seekers is the same as that of the low-field-seekers. At these short times, there are peaks at high spectral shift, indicating a greater number of molecules in high field than in low field. This is due to a greater volume of high-field regions within the cell. After the ablation pulse, the high-field-seeking CaH molecules (the left-hand spectral feature) rapidly leave the trap. This decay is exponential with the same time constant as that of CaH produced with the magnetic trap off (under otherwise similar conditions). We believe this to be the timescale on which the CaH diffuses to the walls, where it sticks.

In sharp contrast to the high-field-seeking distribution, the low-field-seeking distribution changes shape dramatically, and exists for a longer time. The movement of the right-hand-side spectral feature towards lower shifts indicates that the low-field-seeking CaH molecules are moving in towards lower field. The CaH molecules move from their initial spatial distribution to a thermal, trapped distribution, increasing their density by over an order of magnitude. This occurs on the same diffusion timescale as discussed above, as the CaH moves through the helium to reach its equilibrium distribution.

By fitting the observed spectrum to simulated spectra of thermal distributions of trapped molecules, we determine the number and temperature of trapped CaH. Figure 3 shows a spectrum of trapped CaH along with a fit to a simulated spectrum of a thermal distribution of trapped CaH. From this fit, we determine there are 1×10^8 CaH molecules trapped at a temperature of 400 ± 50 mK. The trapped molecules are at a density of 8×10^7 cm^{-3} and are lost from the trap with an exponential decay constant of 0.5 s. They can be observed for longer than 2 s. Comparable production conditions without the magnetic trap produced 3×10^8 CaH molecules at densities of only 4×10^6 cm^{-3}; about 30% of the molecules produced are trapped with a density compression factor of 20. (Quoted numbers and densities are accurate to within a factor of two.)

In addition to the trapping and study of CaH molecules in the ground vibrational state ($|v = 0\rangle$), we were also able to detect $|v = 1\rangle$ molecules at zero field. These vibrationally excited molecules (at an energy of 10^3 cm^{-1} higher than the ground state) are out of thermal equilibrium with the translational degrees of freedom. From these data, were able to determine the vibrational relaxation cross-section between CaH and He as $\sigma_V < 10^{-18}$ cm^{-2} at 0.3–1 K. This cross-section is sufficiently low that it should be possible to magnetically trap these molecules via buffer-gas loading. However, production efficiency of the $|v = 1\rangle$ state was significantly less (typically by a factor of 10–100) than for the $|v = 0\rangle$ state. Due to this low signal, we did not attempt to observe trapping of vibrationally excited molecules.

Vital to the success of buffer gas loading is a small cross-section for 'spin-flip' collisions between the buffer gas (helium) and the molecules to be trapped. A low-field-seeking molecule is in a higher energy state than a high-field-seeking molecule. It has the possibility of relaxing to the high-field-seeking state during a collision. In order for buffer gas loading to work efficiently, this spin relaxation cross section (σ_s) must be much smaller than the elastic cross-section (σ_e). The condition $\sigma_e \gg \sigma_s$ allows kinetic thermalization to take place before spin relaxation. From the measured lifetimes of trapped CaH, we have determined the CaH–He spin relaxation cross-section to be $\sigma_s < 10^{-18}$ cm^2. From the data on diffusive loss (to the walls) of CaH molecules at zero field, the CaH–He elastic cross-section is $\sigma_e \geqslant 10^{-14}$ cm^2, resulting in a ratio $\sigma_e/\sigma_s < 10^4$. As thermalization takes place in ~100 collisions, the condition of small σ_s is well satisfied.

Removal of the buffer gas after trapping should lead to evaporative cooling. The cryopumping procedure we used[13,14] with Cr and Eu takes ~10 s, which is longer than we can currently observe trapped CaH. Improvements in the experiment such as a deeper trap, more efficient CaH production, or higher detection sensitivity would lead to longer observation times, allowing time to pump out the helium. Alternatively, more rapid pumping methods could be developed.

Because our technique relies only on elastic collisions with the buffer gas and on the magnetic state of the species, it should be applicable to many paramagnetic atoms and molecules. Implementation of evaporative cooling could lead to the production of large numbers of ultracold molecules. Immediate applications of this work include high-resolution spectroscopy and studies of cold collisions. Future opportunities may include production of quantum degenerate molecular gases and improved searches for permanent electric dipole moments of elementary particles. □

Received 16 July; accepted 17 August 1998.

1. Anderson, M. H., Ensher, J. R., Matthews, M. R., Wieman, C. E. & Cornell, E. A. Observation of Bose-Einstein condensation in a dilute atomic vapor. *Science* **269,** 198–201 (1995).
2. Davis, K. B. *et al.* Bose–Einstein condensation in a gas of sodium atoms. *Phys. Rev. Lett.* **75,** 3969–3973 (1995).
3. Bradley, C. C., Sackett, C. A. & Hulet, R. G. Bose-Einstein condensation of lithium: observation of limited condensate number. *Phys. Rev. Lett.* **78,** 985–989 (1997).
4. Yu, I. A. *et al.* Evidence for universal quantum reflection of hydrogen from liquid ^{4}He. *Phys. Rev. Lett.* **71,** 1589–1592 (1993).
5. Wineland, D. J., Wieman, C. E. & Smith, S. J. (eds) *Proc. 14th Int. Conf.* (Am. Inst. Phys., New York, 1995).
6. Balakrishnan, N., Forrey, R. C. & Dalgarno, A. Quenching of H_2 vibrations in ultracold ^{3}He and ^{4}He collisions. *Phys. Rev. Lett.* **80,** 3224–3227 (1998).
7. Hinds, E. A. & Sangster, K. in *Time-Reversal—The Arthur Rich Memorial Symposium* (eds Skalsey, M., Bucksbaum, P. H., Conti, R. S. & Gidley, D. W.) 77–83 (Am. Inst. Phys., New York, 1993).
8. Migdal, A. L., Prodan, J. V., Phillips, W. D., Bergeman, T. H. & Metcalf, H. J. First observation of magnetically trapped neutral atoms. *Phys. Rev. Lett.* **54,** 2596–2599 (1985).
9. Ketterle, W. & Van Druten, N. J. Evaporative cooling of trapped atoms. *Adv. At. Mol. Opt. Phys.* **37,** 181–236 (1996).
10. Hess, H. F. *et al.* Magnetic trapping of spin-polarized atomic hydrogen. *Phys. Rev. Lett.* **59,** 672–675 (1987).
11. van Roijen, R., Berkhout, J. J., Jaakkola, S. & Walraven, J. T. M. Experiments with atomic hydrogen in a magnetic trapping field. *Phys. Rev. Lett.* **61,** 931–934 (1988).
12. Doyle, J. M., Friedrich, B., Kim, J. & Patterson, D. Buffer-gas loading of atoms and molecules into a magnetic trap. *Phys. Rev. A* **52,** R2515–R2518 (1995).
13. Kim, J. *et al.* Buffer-gas loading and magnetic trapping of atomic europium. *Phys. Rev. Lett.* **78,** 3665–3668 (1997).
14. Weinstein, J. D. *et al.* Magnetic trapping of atomic chromium. *Phys. Rev. A* **57,** R3173–R3175 (1998).
15. Hess, H. F. Evaporative cooling of magnetically trapped and compressed spin-polarized hydrogen. *Phys. Rev. B* **34,** 3476–3479 (1986).
16. Masuhara, N. *et al.* Evaporative cooling of spin-polarized atomic hydrogen. *Phys. Rev. Lett.* **61,** 935–938 (1988).
17. Bahns, J. T., Stwalley, W. C. & Gould, P. L. Laser cooling of molecules: a sequential scheme for rotation, translation, and vibration. *J. Chem. Phys.* **104,** 9689–9697 (1996).
18. Cote, R. & Dalgarno, A. Mechanism for the production of vibrationally excited ultracold molecules of ^{7}Li$_2$. *Chem. Phys. Lett.* **279,** 50–54 (1997).
19. Band, Y. B. & Julienne, P. S. Ultracold-molecule production by laser-cooled atom photoassociation. *Phys. Rev. A* **51,** R4317–R4320 (1995).
20. Fioretti, A. *et al.* Formation of cold Cs_2 molecules through photoassociation. *Phys. Rev. Lett.* **80,** 4402–4405 (1998).
21. Askar'yan, G. A. Effects of the gradient of a strong electromagnetic beam on electrons and atoms. *Sov. Phys. JETP* **15,** 1088–1090 (1962).
22. Ashkin, A. Trapping of atoms by resonance radiation pressure. *Phys. Rev. Lett.* **40,** 729–732 (1978).
23. Miller, J. D., Cline, R. a. & Heinzen, D. J. Far-off-resonance optical trapping of atoms. *Phys. Rev. A* **47,** R3567–R4570 (1993).
24. Friedrich, B. & Herschbach, D. Alignment and trapping of molecules in intense laser fields. *Phys. Rev. Lett.* **74,** 4623–4626 (1995).
25. Takekoshi, T., Patterson, B. M. & Knize, R. J. *Phys. Rev. Lett.* (submitted).
26. Petrich, W., Anderson, M. H., Ensher, J. R. & Cornell, E. A. Stable, tightly confining magnetic trap for evaporative cooling of neutral atoms. *Phys. Rev. Lett.* **74,** 3352–3355 (1995).
27. Kim, J. *Buffer-gas Loading and Magnetic Trapping of Atomic Europium.* Thesis, Harvard Univ. (1997).
28. Berg, L.-E. & Klynning, L. Rotational analysis of the A-X and B-X band systems of CaH. *Physica Scripta* **10,** 331–336 (1974).
29. Martin, H. Laser spectroscopic investigations of the red band systems of CaH. *J. Mol. Spectrosc.* **108,** 66–81 (1984).
30. Leininger, T. & Jeung, G. Ab initio calculation of rovibronic transition spectra of CaH. *J. Chem. Phys.* **103,** 3942–3949 (1995).
31. Berg, L.-E., Ekvall, K. & Kelly, S. Radiative lifetime measurement of vibronic levels of the $B^2\Sigma^+$ state of CaH by laser excitation spectroscopy. *Chem. Phys. Lett.* **257,** 351–355 (1996).

Acknowledgements. We thank R. Field for discussions on the theory of the Zeeman structure of CaH. This Letter is based on work supported by the US NSF; J.D.W. is supported by an NSF graduate research fellowship.

Correspondence and requests for mateials should be addressed to J.M.D.